An infrared ring around the magnetar SGR 1900+14

S. Wachter[1], E. Ramirez-Ruiz[2], V. V. Dwarkadas[3], C. Kouveliotou[4], J. Granot[5], S. K. Patel[6] & D. Figer[7]

[1]*Spitzer Science Center, California Institute of Technology, Pasadena, CA 91125, USA*

[2]*Astronomy & Astrophysics, 201 Interdisciplinary Sciences Building, Santa Cruz, CA 95064, USA*

[3]*Department of Astronomy and Astrophysics, University of Chicago, 5640 South Ellis Avenue, AAC 010c, Chicago, IL 60637, USA*

[4]*NASA/Marshall Space Flight Center, 320 Sparkman Drive, Huntsville, AL 35805, USA*

[5]*Centre for Astrophysics Research, University of Hertfordshire, College Lane, Hatfield, Herts, AL10 9AB, UK*

[6]*Optical Sciences Corporation, 6767 Old Madison Pike, Suite 650, Huntsville, AL 35806, USA*

[7]*Chester F. Carlson Center for Imaging Science, Rochester Institute of Technology, 54 Lomb Memorial Drive, Rochester, NY 14623, USA*

Magnetars[1,2] are a special class of slowly rotating (period ∼5-12 s) neutron stars with extremely strong magnetic fields (>10^{14} G) – at least an order of magnitude larger than those of the "normal" radio pulsars. The potential evolutionary links and differences between these two types of objects are still unknown; recent studies, however, have provided circumstantial evidence connecting magnetars with very massive progenitor stars [3–5]. Here we report the discovery of an infrared elliptical ring or shell surrounding the magnetar SGR 1900+14.

The appearance and energetics of the ring are difficult to interpret within the framework of the progenitor's stellar mass loss or the subsequent evolution of the supernova remnant. We suggest instead that a dust-free cavity was produced in the magnetar environment by the giant flare emitted by the source in August 1998. Considering the total energy released in the flare, the theoretical dust–destruction radius matches well with the observed dimensions of the ring. We conclude that SGR 1900+14 is unambiguously associated with a cluster of massive stars, thereby solidifying the link between magnetars and massive stars.

Soft gamma repeaters (SGRs) and anomalous X-ray pulsars (AXPs) are the two main classes of objects currently believed to be magnetars. Their characteristic ages, derived from their rotational properties[6], indicate a young population – typically a few thousand years old. Although these spin-down ages must be treated with caution, the relative youth of SGRs and AXPs is supported by the fact that some AXPs are located at the centres of supernova remnants (SNRs). Associations between SNRs and SGRs have also been claimed in the literature, but, unlike the AXPs, the SGRs are offset from the centres of their proposed SNRs, increasing the likelihood of spurious alignment. As a result, the validity of all SGR–SNR associations has been questioned[7]. Both AXPs and SGRs, for example the AXP CXOU J164710.2−455216 (ref.5) and SGR 1806−20 (ref.8), have been linked to clusters of massive stars. The implied progenitor mass of $M \geq 40-50M_{\odot}$ supports theoretical predictions that very massive stars with sufficient metallicity and the corresponding high mass loss can still form neutron stars[9], contrary to the standard evolutionary picture that such massive stars end their lives as black holes.

As part of our systematic study of the circumstellar environments of SGRs and AXPs, we observed the position of SGR 1900+14 using all three instruments onboard the NASA Spitzer Space Telescope in 2005 and 2007. Surprisingly, our 16 μm and 24 μm images (Fig. 1b, c) reveal a prominent ring-like structure that is not detected in our 3.6–8.0 μm observations. A formal elliptical fit to the ring indicates semi-major and semi-minor axes of angular lenghts $\sim$ 36" and $\sim$ 19", respectively, centred at right ascension 19:07:14.32 and declination +09:19:20.0 $\pm$1.0". This coincides with the radio position of SGR 1900+14 (19:07:14.33 +09:19:20.1 $\pm$0.15"), determined from observations of a transient synchrotron source associated with the 1998 giant flare[10]. We re-examined published and archival data of the field around SGR 1900+14 but found no equivalent structure at optical, near-IR, radio or X-ray wavelengths. In particular, the lack of detection in the radio spectrum, to a limit of [11] $L_{332\mathrm{MHz}} \leq 4 \times 10^{29}\ d_{15}^2\ \mathrm{erg\ s^{-1}}$, and the X-ray spectrum, to a limit of $L_{2-10\mathrm{keV}} \leq 2.7 \times 10^{33}\ d_{15}^2\ \mathrm{erg\ s^{-1}}$ (Chandra data archive, http:cxc.harvard.educda), is important in determining the nature of the ring. Here d_{15} parameterizes the distance to the source, according to $d = 15\ d_{15}$ kpc.

The Spitzer images are dominated by the bright emission from two nearby M5 supergiants that mark the centre of a compact cluster of massive stars at a distance of 12–15 kpc[12,13]. Although it has been suggested that SGR 1900+14 is associated with this cluster[12], an alternative distance of 5 kpc has also been suggested, on the basis of the hydrogen column density of its X-ray spectrum[14]. In addition, the SGR is offset by 12" from the cluster centre, and the visual extinction corresponding to the X-ray derived hydrogen column density[11] ($A_V = 12.8 \pm 0.8$) is significantly different from that deduced optically for the cluster stars[12] ($A_V = 19.2 \pm 1$). Considering both possibilities,

we calculated physical sizes for the semi-major and semi-minor axes of the ring of 0.9×0.5 pc, if SGR 1900+14 lies at a distance of ~ 5 kpc, or 2.6×1.4 pc, if it resides at a cluster distance of 15 kpc.

We have constrained the temperature of the material in the ring by first cross-convolving the images with the point spread function of the different arrays. We then measured the flux through fixed apertures at several positions along the ring. The largest source of uncertainty lies in the subtraction of the local background. We derived a temperature of $130 - 150$ K for the material in the ring using a simple black–body fit, and one of $\sim 80 - 120$ K using a more realistic dust model.[15] We caution that the presence of spectral lines or peculiarities in the underlying mid-infrared spectral shape might significantly alter these derived temperatures. For example, Spitzer observations have revealed a shell only visible at 24 μm, where the broadband flux can be entirely attributed to [OIV] line emission[16]. A broad 22 μm continuum feature has also been identified in environments associated with supernovae and massive star formation[17].

The 70 μm image shows a bipolar flux distribution along the minor axis of the ellipse (Fig. 1d). Extended enhancements in the ring are also seen at these positions in the 16 and 24 μm images. Our data do not allow us to determine the underlying three–dimensional geometry of the structure, that is, to distinguish between a limb-brightened shell, a true ring morphology, or a bipolar cavity with equatorial torus. Similarly, an accurate measurement of the total flux in the ring is very difficult because the enveloping diffuse emission (Fig. 1a) coupled with the contribution from the M5 supergiants prohibits a clean separation of the ring emission. Using a narrow elliptical aperture,

we measured fluxes of 1.2$\pm$0.2 Jy and 0.4$\pm$0.1 Jy at 24 μm and 16 μm, respectively, implying ring luminosities of $\nu L_{\nu}(16\mu m) \sim 2\times10^{36}\ d_{15}^{2}\ \mathrm{erg\ s^{-1}}$ and $\nu L_{\nu}(24\mu m) \sim 4\times10^{36}\ d_{15}^{2}\ \mathrm{erg\ s^{-1}}$ (where ν denotes the frequency at which the luminosity is determined).

To test for ring evolution, we used the publicly available MIPSGAL Spitzer Legacy programme observations of the field that were obtained at an epoch (2005 Oct 03) earlier than was our own data set. Creating a difference image from the 24 μm data of the two different epochs, we find no discernable change in the size (positional shifts < 0.5") or flux (root mean square $< 1-2$%) of the ring emission in the 1.6 yr between the two observations. The stationary nature of the ring strongly disfavours one obvious explanation for the creation of the ring – a light echo, due to reprocessing by the surrounding dust, from the 1998 SGR 1900+14 giant flare. This model predicts a typical fractional change in the ring size and brightness between the two epoch observations of $\sim 23\%$, which is not seen in the data (see Supplementary Information for more details).

Morphologically, the ring resembles the wind-blown bubbles and shells observed around evolved massive stars[18–20], such as B supergiants, luminous blue variables and Wolf-Rayet stars. The supersonic wind from the star drives a shock into the surrounding medium, sweeping up the ambient material into a thin, dense, cool shell. The emission from the swept-up material is powered by the luminous central star. Such shells have typical radii of $\sim 2-10$ pc for Wolf-Rayet stars[20] and $0.1-2.3$ pc for luminous blue variables/supergiants[18,19] , overlapping the size of our ring. To guard against a simple chance superposition with an unrelated source, we investigated the photometric properties of stars near the centre of the ring. The sources in the immediate vicinity

of the SGR position[11] are too faint in comparison with the near-infrared luminosities expected for the massive stars discussed above[21,22], and thus cannot be physically associated with the ring. For stars with larger offsets from the centre ($\geq$ 7") we cannot rule out a massive star classification based solely on available archival data. However, a situation in which an off-centre star creates an elliptical ring with an unrelated magnetar at its exact centre appears rather contrived.

In the absence of an obvious chance superposition, the close positional coincidence between the SGR and the centre of the ring then strongly indicates that the SGR and the ring are physically connected. One interpretation is that the ring represents material ejected during the late stages of the SGR progenitor's evolution. However, we know that a supernova explosion occurred, producing the magnetar, and the resulting shock wave is expected to disrupt such a close shell as it interacts with and dissipates into the surrounding material. Some cases are known in which the SNR has over-run a wind-swept shell, but the wind bubble invariably emerges irregular and fragmented in shape after its encounter with the supernova[23]. The symmetric and well-defined appearance of our ring thus would imply that the supernova shock wave is still inside the ring. Our simulations show that this would require the supernova to be < 200 yr old, with bright radio and X-ray emission, contrary to observations. The lack of high-energy X-ray and non-thermal radio emission also excludes the possibility that the observed ring is produced by the emission of the blast wave from the progenitor's supernova explosion.

The rejection of these various possibilities raises the issue of the energy source that is powering the ring. We derived a limit for the required luminosity of the heating source by means of

radiation balance, using the measured temperature $T_{\rm IR}$ of the dust. If the luminosity L_* is dominated by a source of temperature T_*, then (see Supplementary Information for details)

$$L_* \approx 2.7 \times 10^{40} T_{\rm IR}^5 T_*^{-1} R^2 \ {\rm erg\ s^{-1}} \quad (1)$$

where $T_{\rm IR}$ is measured in units of 100 K, T_* is measured in units of 10^4 K and R, the distance from the central heating source, is measured in units of parsecs.

We note that the persistent X-ray luminosity of the SGR is only $L_{2-10\,{\rm keV}} \approx 2.0 - 3.5 \times 10^{35}\ d_{15}^2\ {\rm erg\ s^{-1}} \ll L_*$ and, thus, cannot generate the observed infrared emission from the ring. The only viable heat source consistent with the observed properties of the ring appears to be irradiation from the stars in the nearby cluster. Figure 1a clearly shows that both the cluster and SGR 1900+14 are embedded in a diffuse, extended cloud of 24 μm emission. Similar diffuse 24 μm emission is also observed in association with the clusters containing SGR 1806−20 (ref.24) and Westerlund 1, implying that the extended emission is powered by the cluster stars. We note that, given the location and size of the 24 μm nebula, the cluster might be more spatially extended than previously thought, with as-yet-undiscovered member stars.

A possible mechanism for the creation of the ring is the formation of a dust-free cavity owing to the giant flare activity from SGR 1900+14, which would naturally explain why the ring is centred on the magnetar. The destruction of dust grains can occur either by sublimation due to the heating by ultraviolet[25] or X-ray[26] emission, or by grain charging due to the incident X-rays, which causes the dust grains to gradually shatter into smaller pieces until they are eventually destroyed[26]. The size and shape of the ring can constrain the energy output and degree of anisotropy of the flaring

event (see Supplementary Information for details). Using Equation (25) of ref.26 with the fiducial values and $\alpha = 0$ (where the flux at frequency ν is proportional to $\nu^{-\alpha}$), we find that the dust destruction radius matches well with the observed dimensions of the ring around SGR 1900+14 for $E \geq 6 \times 10^{45} d_{15}^2$ erg. This estimate is close to the observed isotropic equivalent energy[27] in the initial spike of the 27 August 1998 flare; the latter, however, is only accurate for photon energies ≥ 50 keV, whereas the estimated dust-destruction radius requires photons with energies of ~ 1 keV.

Alternatively, a previous, more energetic giant flare from SGR 1900+14, for example, similar to the 2004 December 27 giant flare from SGR 1806-20 (refs 27, 28), with $E \approx 10^{47} d_{15}^2$ erg, could have carved the dust-free cavity during the magnetar's estimated spin-down age of $\sim 1,800$ yr. For a rate of one flare per ~ 50 yr (ref.28), it is reasonable to expect at least one such event $10^3 t_{\rm kyr}$ yr ago, with $t_{\rm kyr} \approx 1$. Then, for the current location of the SGR still to be at the centre of the ring to a precision of 1", the proper motion of the magnetar (due to its birth kick velocity $v_\perp$) and the proper motion of the dust-free cavity (with velocity v_c) should satisfy $\max(v_c, v_\perp) \leq 71 d_{15} t_{\rm kyr}^{-1}$ km s^{-1}.

In light of the probable association between the SGR and the star cluster, we have re-examined the issue of the mismatch in extinction, which has been used as an argument against that connection[11]. As our observations show, the cluster-SGR environment is characterized by a complex dust distribution on small spatial scales and dust destruction by the high-energy emission of the SGR. Because the derived extinction values were based on measurements towards two distinct physical locations (the supergiants and the SGR) and are based on different tracers (gas

and dust) it is then not surprising that the resulting values differ. Similar differences have been observed for the Cas A SNR[29] and extragalactic gamma ray burst sources[30]. In addition, we note that the visual absorption derived solely from the near-infrared photometry of the M supergiants, using both the published data[12] and new measurements extracted from the Two Micorn All Sky Survey, is $A_V = 10.4 - 14.4$ mag, in comparison with $A_V = 19.2 \pm 1$ mag, the value obtained when the optical I band measurement is included. Although this is puzzling and deserves further investigation, the various extinction measurements are clearly subject to large uncertainties and can potentially be reconciled with our conclusion that the SGR is a member of the star cluster.

1. Duncan, R.C. & Thompson, C. Formation of very strongly magnetized neutron stars: implications for gamma-ray bursts. *Astrophys. J.* **392**, L9–L13 (1992)

2. Woods, P.M. & Thompson, C. Soft gamma repeaters and anomalous X-ray pulsars: Magnetar candidates. In *Compact Stellar X-ray Sources* (eds Lewin, W.H.G. & van der Klis, M.) 547-586 (Cambridge Univ. Press, Cambridge, UK, 2006)

3. Figer, D. F., Najarro, F., Geballe, T. R., Blum, R. D., & Kudritzki, R. P. Massive Stars in the SGR 1806−20 Cluster. *Astrophys. J.* **622**, L49–L52 (2005)

4. Gaensler, B. M. et al. A stellar wind bubble coincident with the anomalous x-ray pulsar 1E 1048.1-5937: are magnetars formed from massive progenitors? *Astrophys. J.* **620**, L95–L98 (2005)

5. Muno, M. P., et al. A neutron star with a massive progenitor in Westerlund 1. *Astrophys. J.* **636**, L41–L44 (2006)

6. Kouveliotou, C., et al. An X-ray pulsar with a superstrong magnetic field in the soft γ-ray repeater SGR 1806−20. *Nature* **393**, 235–237 (1998)

7. Gaensler, B. M., Slane, P. O., Gotthelf, E. V., Vasisht, G. Anomalous x-ray pulsars and soft gamma-ray repeaters in supernova remnants. *Astrophys. J.* **559**, 963–972 (2001)

8. Eikenberry, S. S., et al. Possible Infrared Counterparts to the Soft Gamma-Ray Repeater SGR 1806−20. *Astrophys. J.* **563**, L133–137 (2001)

9. Heger, A., Fryer, C. L., Woosley, S. E., Langer, N., & Hartmann, D. H. How massive single stars end their life. *Astrophys. J.* **591**, 288–300 (2003)

10. Frail, D. A., Kulkarni, S. R., Bloom, J. S. An outburst of relativistic particles from the soft gamma-ray repeater SGR 1900+14. *Nature* **398**, 127–129 (1999)

11. Kaplan, D. L., Kulkarni, S. R., Frail, D. A., van Kerkwijk, M. H. Deep radio, optical, and infrared observations of SGR 1900+14. *Astrophys. J.* **566**, 378–386 (2002)

12. Vrba, F. J., et al. The double infrared source toward the soft gamma-ray repeater SGR 1900+14. *Astrophys. J.* **468**, 225–230 (1996)

13. Vrba, F. J., et al. The discovery of an embedded cluster of high-mass stars near SGR 1900+14. *Astrophys. J.* **553**, L17–L20 (2000)

14. Hurley, K., et al. ASCA discovery of an x-ray pulsar in the error box of SGR 1900+14. *Astrophys. J.* **510**, L111–L114 (1999)

15. Draine, B. T. Interstellar dust grains. *Annual Review of Astronomy & Astrophysics* **41**, 241-289 (2003)

16. Morris, P. W., et al. Tentative discovery of a new supernova remnant in Cepheus: unveiling an elusive shell in the Spitzer Galactic First Look Survey. *Astrophys. J.* **640**, L179–L182 (2006)

17. Chan, K. W. & Onaka, T. A broad 22 micron emission feature in the Carina Nebula H II region. *Astrophys. J.* **533**, L33–L36 (2000)

18. Smith, N., Bally, J., & Walawender, J. And in the darkness bind them: equatorial rings, B[e] supergiants, and the waists of bipolar nebulae. *Astronom. J.* **134**, 846–859 (2007)

19. Weis, K. On the structure and kinematics of nebulae around LBVs and LBV candidates in the LMC. *Astron. & Astrophys.* **308**, 67–71 (2003)

20. Gruendl, R. A., Chu, Y.-H., Dunne, B. C., & Points, S. D. A morphological diagnostic for dynamical evolution of Wolf-Rayet bubbles. *Astronom. J.* **120**, 2670–2678 (2000)

21. Crowther, P. A. Physical properties of Wolf-Rayet stars. *ARA&A* **45**, 177–219 (2007)

22. Cox, A. N. 2000, Allen's Astrophysical Quantities, 4th edn (ed. Cox, A. N.) Ch. 7.5 15.3.1 (Springer, New York, 2000)

23. Koo, D.-C., Heiles, C. A fast expanding H I shell in W44: A preexisting wind-blown shell overtaken by a supernova remnant. *Astrophys. J.* **442**, L679–L684 (1995)

24. Wachter, S., Kouveliotou, C., Patel, S., Figer, D., & Woods, P. Spitzer space telescope observations of SGR and AXP environments. *Ap&SS* **308**, 66–71 (2007)

25. Waxman, E. & Draine, B. T. Dust sublimation by gamma-ray bursts and its implications. *Astrophys. J.* **537**, 796–802 (2000)

26. Fruchter, A., Krolik, J. H. & Rhoads, J. E. X-ray destruction of dust along the line of sight to gamma-ray bursts. *Astrophys. J.* **563**, 597–610 (2001)

27. Tanaka, Y. T., et al. Comparative study of the initial spikes of soft gamma-ray repeater giant flares in 1998 and 2004 observed with Geotail: do magnetospheric instabilities trigger large-scale fracturing of a magnetar's crust? *Astrophys. J.* **665**, L55–L58 (2007)

28. Palmer, D. A., et al. A giant gamma-ray flare from the magnetar SGR 1806−20. *Nature*, **434**, 1107–1109 (2005)

29. Hartmann, D. H., et al. On Flamsteed's supernova Cas A. *Nuclear Physics A* **621**, 83–91 (1997)

30. Stratta, G., et al. Extinction properties of the X-ray bright/optically faint afterglow of GRB 020405. *Astron. & Astrophys.* **441**, 83–88 (2005)

Acknowledgements This work is based on observations made with the Spitzer Space Telescope, which is operated by the Jet Propulsion Laboratory, California Institute of Technology under a contract with NASA. Support for this work was provided by NASA through an award issued by JPL/Caltech. This publication also makes use of data products from the Two Micron All Sky Survey, which is a joint project of the University of Massachusetts and the Infrared Processing and Analysis Center/California Institute of Technology, funded by the National Aeronautics and Space Administration and the National Science Foundation. J.G.

gratefully acknowledges a Royal Society Wolfson Research Merit Award. VVD acknowledges support from the National Science Foundation, and useful discussions with R. McCray, A. Crotts and R. Chevalier. D.F. acknowledges support from NASA through the Long Term Space Astrophysics programme, and by the New York State Foundation for Science, Technology, and Innovation Faculty Development Program grant.

Competing interests statement The authors declared no competing interests.

Supplementary information accompanies this paper.

Correspondence Correspondence and requests for materials should be addressed to S.W. (wachter@ipac.caltech.edu).

Supplementary Material for "An infrared ring around the magnetar SGR 1900+14"

Light echo scenario details

If the SGR were surrounded by an extensive dust cloud, a substantial amount of the giant flare radiation will be converted into IR radiation. Given the extended nature of the dust cloud, light travel times across it must be considered. The two MIPS 24 μm images were obtained at $t_1 = 7.10$ yr and $t_2 = 8.75$ yr after the 1998 August 27 giant flare from SGR 1900+14. If the ring is from a light echo due to reprocessing of the giant flare photons then the time delay t is related to the location of the (assumed rapid) reprocessing by $ct = r(1 - \cos\theta)$, where (r, θ, ϕ) are polar coordinates with the SGR located at the origin and with the z-axis pointing to the observer. This locus of points from which reprocessed photons reach the observer simultaneously describes a paraboloidal surface centered on the location of the SGR and symmetric about our line of sight to the SGR, which grows linearly in time, in the sense that r/t is a function of the polar angle θ alone. The lateral distance from the SGR to this surface (at $\theta = 90^\circ$) is simply ct, which corresponds to $ct_1 \approx 2.2$ pc and $ct_2 \approx 2.7$ pc for our two epochs of observation, where ct_1 corresponds to the semi-major axis of the ring for $d \approx 12.5$ kpc.

The main characteristics of such a light echo can be demonstrated by the simple and idealized case of a thin spherical shell of dust of radius R centered on the SGR. Its intersection with the paraboloidal surface described above is simply at $\cos\theta = 1 - ct/R$ so that the apparent ring size

$R_{\rm ring}$ is

$$R_{\rm ring} = R\sin\theta = R\sqrt{\frac{ct}{R}\left(2-\frac{ct}{R}\right)} \qquad 0 < \frac{ct}{R} < 2\,. \tag{2}$$

It initially grows super-luminally, its expansion slowing down until it reaches a maximal size of $R_{\rm ring} = R$ at $t = R/c$, and then begins to shrink increasingly fast until it disappears at $t = 2R/c$. Its apparent velocity $\beta_{\rm app}$ in units of c is

$$\beta_{\rm app} = \frac{1}{c}\frac{dR_{\rm ring}}{dt} = \frac{1-ct/R}{\sqrt{\frac{ct}{R}\left(2-\frac{ct}{R}\right)}} \qquad 0 < \frac{ct}{R} < 2\,. \tag{3}$$

While $\beta_{\rm app} \geq 1$ for much of the time, we also have $\beta_{\rm app} \ll 1$ at $t \approx R/c$, i.e. very close to the time when the ring reaches its maximal size and begins to shrink. However, for two generic observation times one expects a fractional change of $\sim (t_2 - t_1)/t_1$ in the ring size, which in our case corresponds to $\sim 23\%$. Moreover, since the observed ring in our case is elongated with an axis ratio of $\sim 2:1$, the shell of reprocessing dust must clearly be non-spherical, and therefore the maximal size would also depend on the azimuthal angle ϕ, so that the apparent expansion velocity of the ring would never vanish everywhere at once, and one can expect fractional changes of the order of $\sim (t_2 - t_1)/t_1 \sim 23\%$ in the ring shape or brightness between the two epochs, at least in some parts of the ring. Therefore, our strict limits on its exact location, and fractional chances in its size, shape, and brightness (of $< 1 - 2\%$) are very hard to satisfy simultaneously in this scenario.

Dust heating considerations

The temperature of the dust can be used to determine the required luminosity of the heating source by means of radiation balance. If ϵ_λ is the dust absorption efficiency, then its temperature is given

by a balance between the heat input due to the flux it absorbs and emits. If the flux it absorbs is dominated by a point source (which is also a useful approximation for a group of sources at distances larger than their separations) with luminosity L_* peaking at λ_*, at a distance R, then a (spherical, for simplicity) dust grain of radius a absorbs energy at a rate of

$$\dot{E}_{\rm absorbed} = \epsilon_{\lambda_*} \pi a^2 \frac{L_*}{4\pi R^2} \ , \tag{4}$$

and radiates away energy at a rate of

$$\dot{E}_{\rm radiated} = 4\pi a^2 \epsilon_{\lambda_{\rm IR}} \sigma T_{\rm IR}^4 \ , \tag{5}$$

where $\lambda_{\rm IR} \sim hc/kT_{\rm IR}$. Equating the two rates gives:

$$L_* = 16\pi R^2 \left(\frac{\epsilon_{\lambda_{\rm IR}}}{\epsilon_{\lambda_*}} \right) \sigma T_{\rm IR}^4 \ . \tag{6}$$

If the luminosity L_* is dominated by a source of temperature T_* ($\sim hc/k\lambda_*$), and both ϵ_{λ_*} and $\epsilon_{\lambda_{\rm IR}}$ are in the range where $\epsilon_\lambda \propto 1/\lambda$, then

$$\frac{\epsilon_{\lambda_{\rm IR}}}{\epsilon_{\lambda_*}} \sim \frac{T_{\rm IR}}{T_*} = 0.01 \left(\frac{T_{\rm IR}}{100 \ {\rm K}} \right) \left(\frac{T_*}{10^4 \ {\rm K}} \right)^{-1} \ . \tag{7}$$

and

$$L_* = 2.7 \times 10^{40} \left(\frac{T_{\rm IR}}{100 \ {\rm K}} \right)^5 \left(\frac{T_*}{10^4 \ {\rm K}} \right)^{-1} \left(\frac{R}{1 \ {\rm pc}} \right)^2 \ {\rm erg \ s^{-1}} \ . \tag{8}$$

This basically sets a limit for the required heating source. Note that for a given source equation (8) implies that the dust temperature decreases rather slowly with the distance from the source, $T_{\rm IR} \propto R^{-2/5}$ and could help explain why we do not detect a change along the ring in the apparent temperature of the ring emission.

Giant flare energetics and anisotropy

The $\sim 2:1$ axis ratio of the ring suggests that if it was indeed formed by the initial spike of a giant flare, then the flare had an angular variation in its isotropic equivalent luminosity L or energy E of a factor of ≥ 4 (since the sublimation radius scales as $L^{1/2}$ while the dust shattering radius scales as $E^{1/2}$, and the true axis ratio of the dust-free cavity could be somewhat larger than the observed axis ratio of the ring due to projection effects). Moreover, the relatively modest degree of anisotropy suggests that the true total energy output in the event that created the dust-free cavity was $\geq 6 \times 10^{45} d_{15}^2$ erg, which is comparable to the *isotropic equivalent* energy output for the 2004 giant flare from SGR 1806-20. For the latter event it is hard to estimate the true energy output, since we have no observations that directly constrain the emission in directions other than our line of sight.

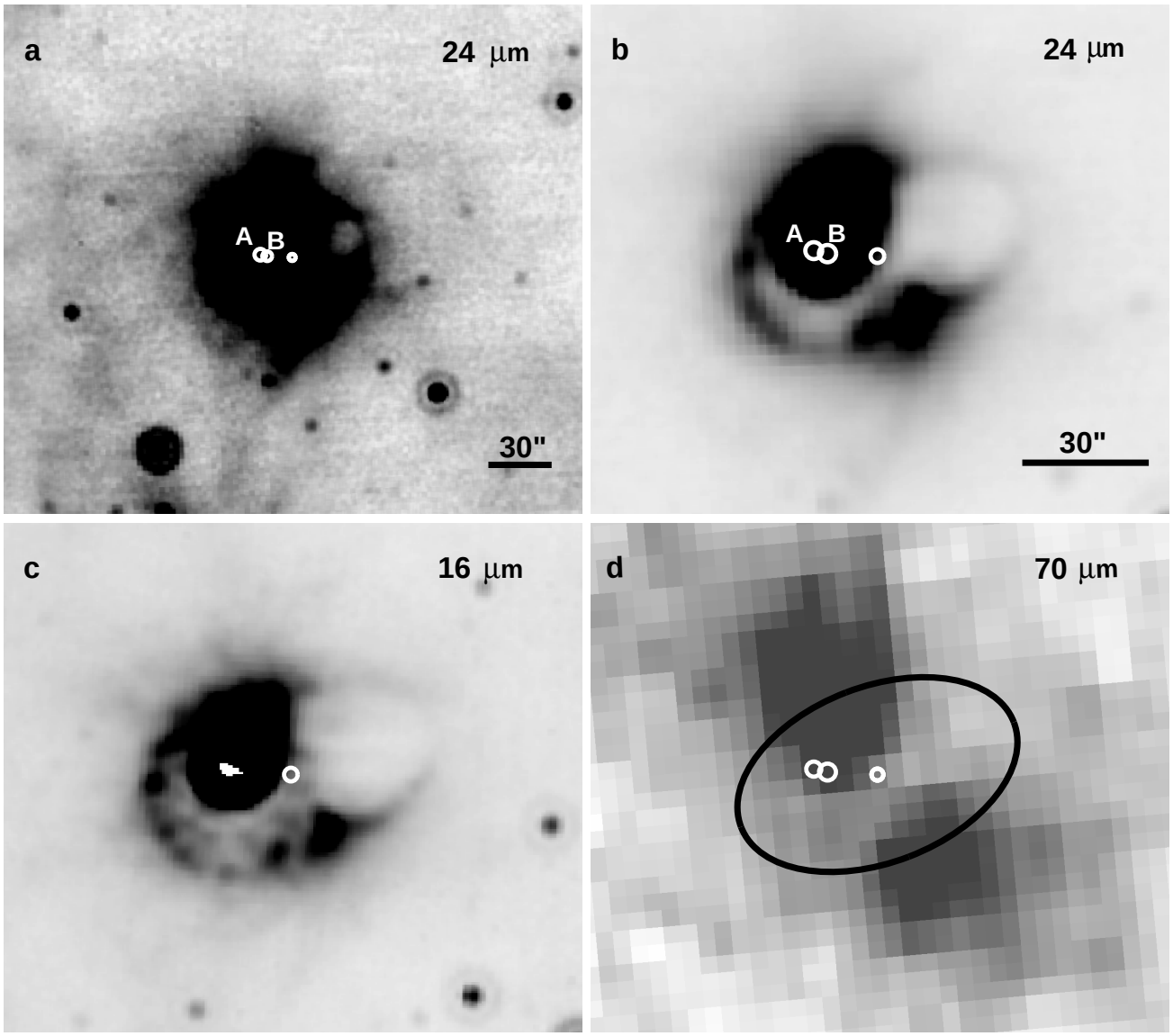
a
24 μm
A
B
30"
b
24 μm
A
B
30"
c
16 μm
d
70 μm

Figure 1 The infrared ring around SGR 1900+14. Spitzer Space Telescope imaging of SGR 1900+14 was acquired on 2005 September 20 using the InfraRed Array Camera (3.6−8.0 μm), on 2005 Oct 11 with the blue (16 μm) peak-up imaging mode of the InfraRed Spectrograph (IRS), and on 2007 May 29 with the Multiband Imaging Photometer for Spitzer (MIPS; $24, 70\mu$m). Only the MIPS and IRS images are shown here. We assembled the basic calibrated data products into combined images using the Mosaicking and Point-source Extraction package. For the MIPS data, we first applied a differential flat field to correct for small (1−2%) instrumental artefacts. The final combined images (**a–d**) have effective exposure times of 31 s for IRS and 16 s for both MIPS channels. The white circle in the centre of each image marks the radio position of the SGR. For all images, north is up and east is to the left. **a**, MIPS 24 μm image scaled to show the diffuse emission enveloping both the SGR and the nearby cluster. The white circles labeled 'A' and 'B' indicate the positions of the red supergiants[12] located at the centre of the star cluster. **b**, Close-up of the MIPS 24 μm image shown in **a**, but scaled to highlight the ring-like structure of the extended emission. **c**, IRS 16 μm peak-up image covering the same field of view as **b**. **d**, MIPS 70 μm image showing emission associated with the enhanced areas along the minor axis of the ellipse also seen at 16 and 24μm. The position of the ring is indicated by the black ellipsoid. The convolution of the 16 and 24 μm images to the resolution of the 70 μm array indicates that the ring emission is too spatially confined and faint to be detectable at this wavelength.